Renal cell carcinoma in children and adolescents: a retrospective study of a French-Italian series of 93 cases

Thomas Denize, Simona Massa, Alexander Valent, Lucia Militti, Alessia Bertolotti, Marta Barisella, Nathalie Rioux-Leclercq, Gabriel G. Malouf, Filippo Spreafico, Arnauld Verschuur, et al.

Denize Thomas (Orcid ID: 0000-0002-8618-7691)
Vujanic Gordan (Orcid ID: 0000-0003-0726-6939)

Renal cell carcinoma in children and adolescents: A retrospective study of a French-Italian series of 93 cases

Running title: retrospective study of 93 pediatric renal cell carcinomas

Thomas Denize [1], Simona Massa[2¶], Alexander Valent[3], Lucia Militti[2], Alessia Bertolotti[2], Marta Barisella[2], Nathalie Rioux-Leclercq[4], Gabriel G. Malouf[5], Filippo Spreafico[6], Arnauld Verschuur[7], Justine van der Beek[8], Lieve Tytgat[8], Marry M van den Heuvel-Eibrink[8], Gordan Vujanic[9], Paola Collini[10*], Aurore Coulomb[1*]

1 – Department of Pathology, Sorbonne Université, Assistance Publique Hôpitaux de Paris – Hôpital Armand Trousseau, Paris, France

2 - Department of Diagnostic Pathology and Laboratory Medicine, Fondazione IRCCS Istituto Nazionale dei Tumori, Milan, Italy

3 - Service de Génétique des tumeurs, Département de Pathologie, Institut Gustave Roussy, Villejuif, France

4 - Department of Pathology, Rennes University Hospital, Rennes, France

5 - Service d'Oncologie Médicale, Institut de Cancérologie de Strasbourg, Strasbourg, France

6 - Pediatric Oncology Unit, Fondazione IRCCS Istituto Nazionale dei Tumori, Milan, Italy

7 - Department of Pediatric Oncology, Hôpital d'enfants de la Timone, Marseille, France

8 - Princess Máxima Center for Pediatric Oncology, and Utrecht University, Utrecht, The Netherlands

9 - Department of Pathology, Sidra Medicine / Weill Cornell Medicine, Doha, Qatar

10 - Soft Tissue and Bone Pathology and Pediatric Pathology Unit, Fondazione IRCCS Istituto Nazionale dei Tumori, Milan, Italy

This article has been accepted for publication and undergone full peer review but has not been through the copyediting, typesetting, pagination and proofreading process which may lead to differences between this version and the Version of Record. Please cite this article as doi: 10.1111/his.14634

9 - Sorbonne Université, Assistance Publique Hôpitaux de Paris – Hôpital Armand Trousseau, Paris, France

¶ present address: Unit of Pathology, Azienda Ospedaliera Specialistica dei Colli Monaldi-Cotugno-CTO, Naples, Italy

* These authors contributed equally to this work

Corresponding author: Aurore Coulomb, Department of Pathology, Sorbonne Université, Hôpital Armand Trousseau, 26 Avenue du Dr Arnold Netter, 75012 Paris, France

Email: Aurore.coulomb@aphp.fr

Conflicts of interests: authors have no COIs to declare

Word count: 5618

Abstract

Background: Renal cell carcinomas represent 2 to 5% of kidney malignancies in children and adolescents. Appropriate diagnostic and classification are crucial for the correct management of the patients and in order to avoid inappropriate preoperative chemotherapy, which is usually recommended if a Wilms tumor is suspected.

Methods: a French-Italian series of 93 renal cell carcinomas collected from 1990 to 2019 in patients aged less than 18 years old was reclassified according to the 2016 WHO classification and the latest literature. *TFE3* and *TFEB* FISH analyses and a panel of immunohistochemical stains were applied.

Results: The median age at diagnosis was 11 years (range: 9 months – 17 years). *MiT* family (*MiTF*) translocation renal cell carcinomas accounted for 52% of the tumors, followed by papillary renal cell carcinomas (20%) and unclassified renal cell carcinomas (13%). Other subtypes, such as SDHB-deficient and Fumarate hydratase-deficient renal cell carcinomas, represented 1 to 3% of the cases. We also described a case of *ALK*-rearranged renal cell carcinoma with a metanephric adenoma-like morphology.

Conclusion: A precise histological diagnosis is mandatory as targeted therapy could be applied for some RCC subtypes, i.e., *MiTF*-translocation and *ALK*-translocation renal cell carcinomas. Moreover, some RCC subtypes may be associated with a predisposition syndrome that will impact patients' and family's management and genetic counseling. A precise RCC subtype is also mandatory for the clinical management of the patients and the inclusion in new prospective clinical trials.

Keywords: Renal cell carcinoma, Pediatric cancer, TFE3

Introduction

Renal malignancies in children and adolescents are mainly represented by Wilms tumors (WTs). In contrast with adults, in which renal cell carcinomas (RCCs) represent more than 80% of kidney tumors, RCCs account for only 2-5% of kidney tumors in the pediatric population (1–3). The 2016 WHO Classification of Tumors of the Urinary System and Male Genital Organs, mainly based on adult series, categorizes renal cell tumors into 16 definitive subtypes and four emerging entities (4). In the meantime, new developments in WHO entities occurred, in particular in papillary RCC (PRCC) classification (5,6). In fact, PRCCs could be better subclassified into 'type 1' and 'others, NOS', being the former category of 'PRCC type 2' considered as a miscellanea of heterogeneous, mainly high-grade PRCCs. Microphthalmia Transcription (*MiT*) family - translocation RCCs (*MiTF*-TRCCs) represent 40-49% of RCCs in children and 1.6-4% in adults (7,8). In adults, compared to children and adolescents, these tumors tend to be more aggressive and have more nodal metastases (9). The prognostic value of metastatic lymph nodes in children is unclear, with contradictory data in the literature (10–12). Exposure to cytotoxic chemotherapy in early childhood (especially for neuroblastoma or brain tumors) is a known risk factor for *MiTF*-TRCC (13). More recently, a series of three *MiTF*-TRCC in patients with chronic kidney disease and long-term exposure to immunosuppressive therapy was reported (14).

In a few large pediatric series (15–22), non-*MiTF*-TRCCs are represented mainly by PRCC type 1 and 2 and clear cell RCC (CCRCC). Recently, some new entities have been described, such as the eosinophilic solid and cystic RCC (ESCRCC) (23), which has also been reported in three children (24).

Adult RCCs may be related to hereditary predisposition syndromes in 5% of the cases (25). Early age of RCC onset seemed to be a predictive factor of hereditary syndromes, but the prevalence in children and adolescents is unknown. To date, 15 RCC predisposition syndromes have been described, the most frequent being von Hippel-Lindau disease (VHL), Birt-Hogg-Dubé (BHD), and Tuberous Sclerosis Complex (TSC) (26). The 2016 WHO classification introduced two new entities arising in a peculiar genetic setting, including the succinate dehydrogenase deficient RCC (SDH-deficient RCC) and fumarate hydratase deficient renal cell carcinomas (FH-deficient RCC). SDH-deficient RCCs are related to the pheochromocytoma/paraganglioma predisposition syndrome, which is well known in pediatrics due to the occurrence of paraganglioma in this age group. FH-deficient RCCs are related to the hereditary leiomyomatosis and renal cell cancer syndrome (4).

Since RCC incidence increases with advancing patient age in respect to WT, in general, a needle core biopsy is strongly recommended in children above 10 years of age prior to any medical treatment (27–30). Accurate tumor classification is required to avoid unnecessary preoperative chemotherapy and possibly perform nephron-sparing surgery in smaller RCCs, which has shown to have a good outcome in small pediatric series (31,32). Accurate diagnosis may also allow the inclusion of patients in trials addressing the role of targeted therapies in patients with metastatic or unresectable disease. Indeed, of 53 patients with translocation carcinoma treated with either anti-vascular endothelial growth factor receptor inhibitors or mammalian target of rapamycin inhibitors, seven achieved objective response (33). Additionally, two patients with stage 4 *MiTF*-TRCC were treated with anti-MET tyrosine kinase inhibitors and showed disease control for 15 months (34).

This study aimed to reclassify a large French and Italian series of 93 RCCs from 1990 to 2019 in children and adolescents up to 18 years of age according to the 2016 WHO classification and the latest literature, to provide an updated histopathologic overview of the RCC landscape in this age group.

Materials and methods

The cases, which included children up to 18 years of age diagnosed with RCC between 1990 and 2019, were retrieved from the archives of the Department of Pathology, Armand Trousseau Hospital of Paris, France, and of the IRCCS Istituto Nazionale dei Tumori of Milan, Italy. It was approved by the Ethics Committee of the IRCCS Istituto Nazionale dei Tumori of Milan, Italy, 23 September 2014, amendment n. 3 to the study INT 14/03 'Wilms tumor: diagnostic - therapeutic protocol AIEOP 2003'. This study was performed in accordance with the declaration of Helsinki.

Only cases with available histologic material for immunohistochemical and FISH analyses for reclassification were included in this study. Ninety-three cases were suitable for all the analyses. The 42 Italian cases were registered in the Italian CNR92 and AIEOP TW2003 Protocols, or in the Pediatric Renal Tumor Registry of the AIEOP TW2003 Protocol. Ten French cases out of 51 were included in the SIOP-RTSG 93-01 and 2001 Protocols (20). The clinicopathologic variables registered were age at diagnosis, gender, type of surgery, tumor size, multifocality, architecture, cytology, WHO/ International Society of Urological Pathology (ISUP) grade, presence of inflammation, necrosis, calcifications, bone metaplasia, capsular invasion, and vascular invasion. All the available slides stained with hematoxylin and eosin (HE) or hematoxylin, eosin, and saffron (HES) were reviewed by four pathologists (AC, PC, SM, and TD). Of these, a formalin-fixed paraffin-embedded (FFPE) block was

selected for FISH and immunohistochemical analyses for each case. Tumors were reclassified according to the 2016 WHO classification and the subsequent literature (4–6) along with morphology, immunophenotype, and FISH analyses for *TFE3* in all cases. The group of PRCCs was subdivided into PRCC type 1 and PRCC, NOS, high grade. Additional molecular studies (*TFEB, ALK, and VHL* FISH analyses, and NGS mutational and gene fusion transcript analyses) were added when appropriate in selected cases (morphology suggestive of *TFEB*-TRCC, ALK-immunoreactivity, loss of SDHB expression, unclassified cases).

Immunohistochemistry

Five-micron tissue sections were cut from the selected block. Immunostaining assays were performed on a Leica Bond Platform (Leica Microsystems, Chicago, IL, USA) for French cases and an automated DAKO Immunostainer for Italian cases. The antibodies were used according to the manufacturer's protocol. The same panel of antibodies was applied to all cases. The antibodies/antisera used are listed in Table 1. A stain was considered 'positive' when at least 5% of neoplastic cells showed immunoreactivity in the appropriate site.

FISH analyses

Fluorescence in situ hybridization (FISH) analyses were performed on selected areas of whole sections of all cases. In case of focal TFE3 and TFEB immunoreactivity, the analysis was performed on the positive foci. FISH analysis for the *ALK* gene was performed in cases found ALK-positive on immunohistochemistry. FISH analysis for the VHL gene was performed in 2 cases of clear cell RCC

(CCRCC). On a 3-μm thick formalin-fixed paraffin-embedded tissue section, analyses were performed by counting at least 100 tumor cells in an area selected by pathologists. For the *TFE3* gene at Xp11.2 and *ALK* gene at 2p23, commercially available Zyto*Light* ® SPEC *TFE3* Dual Color Break Apart Probe and LSI *ALK* Dual Color Break Apart Rearrangement Probe were used according to manufacturer's instructions with appropriate modifications. For the *TFEB* gene at 6p21.1, bi-color custom probes prepared in the laboratory using the library RP11 localized on 6p21.1 and framing the *TFEB* gene were used. For the *VHL* gene, a commercially available SPEC VHL (3p25.3)/CEN3 from Zytovision was used. Methods of FISH analysis are described in Supplementary File 1.

Mutational analysis

Mutational analysis for SDHB was performed using Targeted NGS Ion Torrent Magic Panel (Life Technologies). Mutational analysis for *TSC1/TSC2* was performed using targeted NGS using a panel custom DRAGON (Agilent). ALK fusion detection was performed by using the Oncomine Comprehensive Assay Plus RNA (Thermofisher) containing a targeted multi-biomarker panel that enables the detection of known and novel fusions from 49 genes. Manual preparation of library and sequencing on the Ion Gene Studio S5 system were performed following standard procedures.

Results

Clinical features

In total, 93 cases were identified from 1990 to 2019, including 46 boys and 47 girls (sex ratio 1:1). The median age at diagnosis was 11 years (range: 9 months - 17 years). Nine patients (10%) had been previously treated with chemotherapy for other malignant tumors (two WT, one non-Hodgkin lymphoma, one medulloblastoma, three acute lymphoblastic leukemia, one rhabdomyosarcoma, one without information). Other pre-existing noticeable diseases included, in one case each: chronic renal failure, hemolytic and uremic syndrome, tuberous sclerosis complex, *TSC2/PKD1* contiguous gene syndrome, sickle cell disease, and celiac disease. One patient had a horseshoe kidney, and three patients had multiple renal cysts. Tumors were unilateral and unifocal in 82 cases, multifocal in 9, and bilateral in 2. The type of surgery was known for 79 patients (85%): 12 (15%) patients underwent nephron-sparing surgery (6 left, 6 right), and 67 (85%) patients underwent a radical nephrectomy (39 left, 28 right). Lymph nodes were sampled in 49 (53%) patients. Of these, 15 (30%) had at least one nodal metastasis (range 1-17 metastases). Twenty-seven patients (29%) had a previous needle biopsy to assess the tumor type, and two of them had seeded in the biopsy tract. Tumor size was known for 91 tumors, with a median diameter of 5.5 cm (range, 1.2-27cm).

Case series

RCC subtypes and frequency are detailed in Table 2. The immunohistochemical profiles are detailed in Table 3.

Immunohistochemical expression of TFE3 was present in all *TFE3* rearranged cases and in 15/52 (28%) of *TFE3* not rearranged RCCs (sensitivity 100%, specificity 72%

for TFE3-TRCC). In older cases, immunoreactivity occurred mostly in the outer part of tumor sections.

MiTF translocation RCC (MiTF-TRCC) (48 cases)

Thirty-nine tumors displayed a *TFE3* rearrangement, and six tumors a *TFEB* rearrangement at FISH analysis. For three other patients, the FISH analysis failed due to ancient FFPE material. On the basis of a typical morphology and immunophenotype, two of these cases were classified as *TFE3*-TRCC and one case as *TFEB*-TRCC. In all case series, both rearranged and non-rearranged cases showed neither *TFE3* nor *TFEB* amplification.

In the *TFE3*-TRCC group, patients were females in 27 cases and males in 14 cases (F/M ratio=2:1). Median age at diagnosis was 11 years (range: 9 months-17 years). Four patients (10%) had a known history of chemotherapy, and one had chronic renal failure. Twenty-three (56%) patients had a diagnostic needle core biopsy, and two (9%) relapsed on the tract and subsequently died of the disease. Of the surgical specimens, 31/41 (76%) had sampled lymph nodes, 21 (68%) of whom were metastatic. Median tumor size was 5.5cm (range 2 to 13.5 cm).

Histologically, the main architectural pattern was papillary, with mostly short and thick papillae (Fig 1a, 1b, 1c). In 27 cases, there was an admixture of tubular and nested patterns. In five cases, solid sheets of cells were also observed (Fig 1d, 1e).

In all cases, the cytoplasm was either clear or an admixture of clear and granular eosinophilic (Fig 1f). Nuclei were mainly high grade according to the WHO/ISUP grading system with 37/41 (90%) WHO/ISUP grade 3, whereas two cases were WHO/ISUP grade 2 and 2 cases WHO/ISUP grade 4. In 26 cases, the tumor was

surrounded by a capsule, which was invaded in 12 cases. Vascular invasion was observed in 18 (44%) tumors. Tumoral necrosis of 5% to 75% of the tumor surface was present in 69% of cases. Calcifications were observed in 26 (63%) cases and bone metaplasia in 2 (5%) cases. Regarding the immunoprofile, TFE3 was strongly expressed in all cases. HMB45 and Melan-A were expressed in 6/36 and 2/35 cases, respectively. (Fig1g). AMACR was expressed in all cases (Fig 1h). CAIX was expressed in 16/33 cases in a focal fashion (Fig1i), CK7 in 11/37, and CK19 in 11/31 (table 3). *TFE3* FISH showed a split-apart signal in 39 cases and failed in two cases due to ancient FFPE material.

In the *TFEB*-TRCC group, there were five boys and two girls, ranging from 4 to 15 years of age. Tumors measured 3 to 14 cm. One patient had neoadjuvant chemotherapy. One of the two patients with hilar lymph nodes samples on the surgical specimen had lymph node metastasis. The architecture was polymorphic with nested, papillary, tubular, cystic, and solid areas (Fig 2a, 2b, 2c, 2d). The cytoplasm ranged from clear to eosinophilic in most tumors, apart from one tumor that was only composed of large clear cells (Fig 2e, 2f). Four tumors were encapsulated with one capsular invasion. Calcifications were found in one case, and there was scarce necrosis in two cases. Tumoral cells focally expressed CD10 (Fig 2g), while HMB45 (Fig 2h) and Melan-A were expressed in 6/7 and 7/7 cases, respectively (Fig 2i). *TFEB* FISH showed a split-apart signal in 6/7 cases. It failed in a case due to a 20-year-old FFPE material.

Papillary RCC (PRCC), NOS, high grade (10 cases):

Patients were aged 6 to 16 years (median age: 10 years). One patient with a contiguous gene syndrome (*TSC+PKAD1* microdeletion) developed a contralateral

PRCC, NOS, high grade four years after the first tumor resection. Tumors measured 1.2 to 13.5 cm. They were predominantly of papillary architecture, with some solid foci in one case. The cytoplasm was eosinophilic in all the cases (Sup Fig 1b), being one of them diagnosed as oncocytic PRCC (Fig 3a and Sup Fig 1c). In all tumors, the WHO/ISUP grade was 3. Necrosis was present in 5 tumors (55%). Six tumors were encapsulated (66%). AMACR was consistently positive in all cases, and CK7 and CK19 in 7/10 and 6/8 cases, respectively (Table 3). The oncocytic PRCC expressed AMACR, but CK7, CAIX, and vimentin were negative. FH and SDHB expression were retained in all cases, and *TFE3* FISH was negative.

Papillary RCC (PRCC), type 1 (9 cases):

Patients were aged 3 to 17 years (median age of 9y). In one case, the tumor was multifocal. The tumors measured from 2 to 11 cm, and 8 out of 9 tumors were encapsulated. All tumors were alike, with predominant thin papillae lined by small clear to eosinophilic cells (Sup Fig 1a). The nuclei were mostly low grade, WHO/ISUP grade 2 being the most common (four tumors were WHO/ISUP grade 2, three WHO/ISUP grade 1, and two WHO/ISUP grade 3).

Necrosis was a common feature (6/9 cases) and represented up to 95% of the tumor surface. Calcifications were also seen in six cases. Regarding their immunoprofile, CK7 was strongly expressed in 100% of the cases. AMACR was expressed on 6/7 cases and CK19 on 3/5 (Table 3). *TFE3* FISH was negative in all cases.

Clear cell RCC (CCRCC) (4 cases):

Patients were two girls aged 8 and 12 years and two boys aged 16 and 17 years. Two of them had a history of contralateral Wilms tumors. The CCRCC tumors

measured 1.5 to 11 cm (mean 5cm). Two cases displayed a classic adult-type clear cell RCC morphology with a WHO/ISUP grade 2. Based on morphology, two cases were suspected of being CCPRCC. The typical immunoprofile confirmed the obvious cases and corrected the diagnosis on the suspected CCPRCC. (Fig 3c, 3d, 3e, 3f). FISH analysis revealed VHL deletion in one case. Follow-up data showed that all patients were alive 7 years after the diagnosis,

Chromophobe RCC (3 cases):

Patients were two girls (age 6 and 15 years) and one boy (age 15 years). The tumors measured between 4.3 and 9.5 cm. They were composed of nests or trabeculae of eosinophilic cells with granular cytoplasm and well-demarcated cell membranes (Fig 3b). The nucleus was often irregular with perinuclear clearing. Binucleations were also observed. Two of the tumors were encapsulated. Immunohistochemical analysis showed a strong CK7 expression in all the cases and CD117 expression in two cases. Vimentin was negative in all cases.

ALK-TRCC (2 cases):

Two boys aged 10 and 12 years, without any history of sickle cell disease, were diagnosed with *ALK*-translocation associated RCC. The tumors measured 5 and 10 cm, respectively. Follow-up was available for one patient who developed lung metastasis. One case presented sheets and cords of eosinophilic/oncocytic syncytial cells with moderate nuclear polymorphism (Fig 3g, 3h). In this case *VCL* (exon 6) :: *ALK* (exon 20) gene fusion transcript was detected. The other case was solid, cystic and composed of small, clear to eosinophilic cells with low-grade nuclei, with a metanephric adenoma-like morphology. This case showed a *non-VCL::ALK* gene

fusion transcript. Both tumors were encapsulated and presented capsular invasion. Numerous calcifications were observed in both cases, as well as a dense inflammatory infiltrate.

ALK was consistently expressed in the cytoplasm with membranous reinforcement (Fig 3i). CK7, AMACR, Vimentin, keratins CAM5.2, and EMA were expressed in the two cases and CAIX in one of the cases. INI1/SMARCB1 was retained (Table 3).

FISH analysis for *ALK* gene showed a split-apart signal in both cases.

Collecting duct carcinoma (1 case):

The patient was a 17-month-old boy without sickle cell disease. The tumor occupied the whole left kidney with lymph node metastasis. It was mainly composed of large eosinophilic and atypical cells organized in tubules, isolated cells, or small sheets (Sup Fig 1d). The proliferation widely infiltrated the renal parenchyma, the surrounding fat tissue, and the adrenal gland. Areas of sarcomatoid morphology were observed, as well as necrosis and vascular invasion. A marked immune infiltrate was observed. CK7, CK19, and 34betaE12 keratin were expressed. CAIX and AMACR were negative (Table 3). INI1/SMARCB1, FH, and SDHB expression were retained., and *TFE3* FISH was negative.

Renal medullary carcinoma (1 case):

A 14 years-old boy with sickle cell trait and type 2 neural ceroid lipofuscinosis developed an 8 cm right renal mass with nodal and adrenal metastasis. He was lost at follow-up after developing liver metastasis. On microscopic examination, the tumor was composed of trabecular or small sheets of atypical cells with high mitotic activity and numerous apoptosis (Sup Fig 1e). The tumor developed in a fibrous stroma

infiltrated by a polymorphous inflammatory infiltrate. CK7, CK19, 34betaE12 keratin (focal), AMACR, and CD117 were positive. There was a loss of expression of INI1/SMARCB1 (Sup Fig 1f) (Table 3).

Succinate De-Hydrogenase (SDH)B-deficient RCC (1 case):

A 10-year-old boy was diagnosed with a 3.5 tumor on the right kidney. This patient had a Kaposiform hemangioendothelioma 10 years prior to developing the kidney tumor and was treated with interferon-alpha. The tumor presented with an acinar architecture with eosinophilic cells with low-grade nuclei (Fig 4a, 4b). The acini were separated by a mucinous stroma with hemorrhage. The tumor was well delimitated but not encapsulated. Vimentin, AMACR, and CD10 were expressed, whereas CAIX, CK7, and CD117 were negative. SDHB expression was lost (Fig 4c).

A loss of function pathogenic germinal mutation of *SDHB* (c.744C>G, p.248N>K, exon 7) was detected by NGS. No genetic counseling was performed.

Fumarate Hydratase (FH)-deficient RCC (1 case):

A 14-year-old boy developed a 17 cm left renal tumor involving the whole kidney. An invaded lymph node was resected along with the kidney. The patient did not present any medical condition or history of chemotherapy. His maternal grandmother died of renal cell carcinoma aged 47 years. The patient died of metastatic dissemination to the lungs, lymph nodes, and bones 17 months after surgery. No germline genetic analysis was performed at that time. On microscopic examination, the tumor has a tubular-papillary architecture with microcystic changes, micropapillae and acinar formations, as well as solid sheets. The cells were lightly eosinophilic (Fig 4d). The nuclei were organized in a pseudostratified fashion. The nucleoli were cherry red,

with perinucleolar clarification, and were visible at 10x magnification (Fig 4e). Lymphovascular invasion was noted. Necrosis was present on 10% of the surface of the tumor. Calcifications were observed, as well as a slight lymphocytic infiltrate. AMACR immunohistochemistry was strongly positive in all cells, while CK7 was negative. There was a loss of expression of FH in tumor cells (Fig 4f).

Unclassified RCC (13 cases):

Thirteen children (aged 5 to 16 years) were diagnosed with unclassified RCC. Ninety percent of tumors measured more than 4 cm (range 2.4 cm to 10 cm), and all showed a high nuclear grade. The architectural patterns and cell morphology largely varied among tumors (Sup Fig 1g, 1h, 1i). Necrosis was present in 3 cases, calcifications in 6 cases, and bone metaplasia in 2 cases. Eight cases presented with an inflammatory infiltrate. The immunoprofile was as diverse as the morphology, and they did not fit in any of the 2016 WHO Classification categories. *TFE3* FISH was negative in all cases. One unusual case occurred in an 8-year-old girl without a history of TSC as a 6 cm encapsulated tumor on the left kidney. The tumor was limited to the kidney without nodal involvement and was mainly solid with tubules and acini of eosinophilic granular cells (Fig 4g). Cystic components accounted for 15% of the tumor surface and were lined by large plump eosinophilic cells. The nuclei were round with prominent nucleoli. Numerous multinucleated cells were observed, as well as mast cells. Scarce calcifications were present, but not necrosis. Vimentin and AMACR were diffusely expressed (Fig 4h), as well as CD10 with a typical apical pattern (Fig 4i), while CK20 was negative. FH expression was retained. As this pattern could suggest an Eosinophilic Solid and Cystic RCC (ESCRCC), DNA

sequencing was performed. No *TSC1*, *TSC2,* or *MTOR* mutation was found. This girl was alive and free of disease 111 months after surgery.

Discussion

This series represents a large cohort of RCC in children and adolescents up to 18 years of age with comprehensive up-to-date morphological, immunohistochemical, and FISH analyses and subtyping according to the 2016 WHO classification and the more recent literature (4–6). *MiTF*-TRCC, in particular *TFE3*-TRCC, is the most represented subtype of pediatric RCC as reported in the literature (4). We used TFE3 immunohistochemistry on all cases as a screening method. This approach worked well since TFE3 immunohistochemistry resulted very sensitive in detecting all *TFE3*-rearranged cases. However, specificity was not as high since 15 cases without rearrangement or amplification also showed TFE3-reactivity. Along these lines, while TFE3 immunohistochemistry is a valid screening method, *TFE3* gene FISH analysis resulted in the best method to assess the occurrence of translocation, in keeping with the literature (5,35,36). In this pediatric series, the occurrence of translocation of the *TFE3* gene paralleled a distinct cellular type, that is large cells with high-grade vesicular nuclei and clear eosinophilic granular cytoplasm, present in all our cases. Since it is well known that morphology can also be confusing (37), TFE3 immunohistochemistry followed by FISH analysis in positive cases should be performed on every case of RCC to avoid as much misclassification as possible.

In agreement with the literature, *MiTF*-TRCC represents the main subtype of RCC in our series, with 52% of the cases (4–6,37). The reclassification of RCCs applying updated criteria including comprehensive immunohistochemistry panel and *TFE3* and *TFEB* FISH analyses led to a different distribution of RCC subtypes, with fewer pediatric RCCs classified as PRCC, NOS, high grade (ex type 2) or unclassified RCCs. In our *MiTF*-TRCC subgroup we observed a female predominance (M:F = 1:1.5), mostly in the *TFE3*-TRCC cases. This finding could be explained by the

localization of the fusion partner on the X chromosome. Previous exposure to chemotherapy is reported in this subtype in up to 15% of patients (13). Indeed, in our series, 10% of patients with *TFE3*- or *TFEB*-TRCC had a previous history of chemotherapy. *MiTF*-RCC have also been reported in three children with chronic kidney disease (14), as in one patient in our series. Interestingly, in our series, non-TRCC were not associated with previous chemotherapy or chronic kidney disease. Lymph node metastases were present in 68% of *MITF*-TRCC patients whose lymph nodes were sampled during surgery (noteworthy up to 47% of the patients had no lymph nodes sampled), whereas distant metastases were rare. In the Children Oncology Group Study AREN03B2, 41.1% of *MiTF*-TRCC patients had nodal metastasis and 10.7% distant metastasis (38). In the SIOP-RTSG ongoing study, total regional lymphadenectomy is recommended, given the high incidence of lymph node invasion in *MiTF*-RCC. Moreover, relapses may occur even after many years, as illustrated by one patient in our series who relapsed 19 years after surgery and died due to metastatic spread of the disease. This fact emphasizes the importance of surgical removal of the tumors and lymph nodes and a need for a very long follow-up of children with *MiTF*-RCC.

Notably, in two TFE3-RCC cases among the 29 patients who had a needle biopsy at diagnosis, recurrence on the biopsy tract was observed requiring additional surgical resection. Both patients subsequently developed disseminated disease and died.

In the literature, there is no general agreement on the best diagnostic approach for TFE3-TRCCs (35). We applied TFE3 immunohistochemistry as a screening method to detect *TFE3*-TRCC, followed by FISH analysis. This approach worked well since TFE3 immunohistochemistry was 100% sensitive and 72% specific in detecting *TFE3*-rearranged cases at FISH analysis. TFE3 immunohistochemistry was a quick

and inexpensive screening method, valid at least in the vast majority of cases, in keeping with the literature (35,36). FISH analysis fails to detect few translocations and further molecular methods are necessary for a proper diagnosis (5,35). Though, these other methods are more expensive and not always available in all laboratories. In our pediatric series, *TFE3*-TRCC showed the classic morphology characterized by a solid and papillary architecture with large cells with high-grade vesicular nuclei and clear to eosinophilic granular cytoplasm and frequent psammoma bodies (4). With the more frequent application of TFE3 immunohistochemistry coupled with FISH and/or molecular analysis, *TFE3* rearrangements were also detected in cases of RCC without a classic morphology, mainly in adults (37). We could tentatively suggest the existence of a 'pediatric-type TFE3-TRCC', with a classic morphology. With larger studies on pediatric series, the occurrence of non-classic morphologies also in children could be tested. The presence of calcifications on imaging could also prompt pediatric radiologists to evoke this diagnosis. However, in our series, calcifications and even bone metaplasia were observed in MiTF-TRCC and other RCC subtypes. Tumor size is not different between *MITF*-RCC and non-*MiTF*-RCC in our series. An interesting finding is the low and focal cytokeratin expression in *MiTF*-TRCC. This is useful to classify this tumor correctly. Scarce expression of keratin 7 distinguishes this tumor from PRCC type 1, which strongly expresses cytokeratin 7, but not from PRCC type 2. Unlike *TFE3*-TRCC, *TFEB*-TRCC tumors have a male predominance (9,39). They are less frequent and display a different and peculiar phenotype with a more nested and solid architecture with peripheral lymphocytic infiltrate and frequent expression of melanocytic markers. All our cases expressed Melan-A, while HMB45 was expressed only in some cases, as described in the WHO classification (4).

We report four cases of CCRCC. Two of them presented with a morphology suspect of CCPRCC, but the absence of CK7 expression excluded the diagnosis (4).

In the literature, the youngest patient with FH-deficient RCC (or Hereditary Leiomyomatosis Renal Cell Carcinoma (HLRCC) Syndrome-associated Renal Cell Carcinoma) was an 11-year-old asymptomatic patient who was later diagnosed with an *FH* germline mutation (40–45). In our series, a 14-year-old patient had an FH-deficient RCC, a term used to characterize RCC associated with a loss of FH expression using immunohistochemistry, without known germline mutation in the family. With lung and lymph node metastatic spread at diagnosis, this 14-year-old patient followed the known aggressive tumor evolution without response to treatment, as underlined by Muller and al. (42). As 10 to 30% of HLRCC patients may develop an RCC (40–45), an accurate diagnosis is crucial in order to improve the understanding of oncogenesis and tumor progression mechanisms of this high-risk tumor and to refer the family to genetic counseling.

SDHB-deficient RCC is also associated with a hereditary predisposition syndrome. Of all the mutations associated with the development of hereditary pheochromocytoma/paraganglioma, mutations in all the SDH mitochondrial unit proteins have been associated with a distinct type of renal cell carcinoma, SDHB unit protein being the most frequent (46–48). To date, all the cases arose in a setting of a germline mutation. These tumors are rare, mostly small, and limited to the kidney, but up to 30% of cases are bilateral. Our patient was a 10-year-old boy with a unilateral tumor showing a classical morphology with loss of SDHB expression by immunohistochemistry and an *SDHB* loss of function mutation on NGS. This patient was not sent to genetic counseling.

Less than 40 ALK-rearrangement-associated RCC have been reported in the literature (49). These cases have been mainly described in adults, showing heterogeneous morphologies with a polymorphous papillary, solid, and cribriform architecture within a myxoid stroma, variable fusion partners, being in part associated with sickle cell disease. As in our series, many cases have been discovered using ALK immunohistochemistry as a screening method, followed by FISH and/or molecular confirmation (49). In the reported pediatric subgroup (up to 18 years of age) of 8 cases, the tumor was generally located in the medulla/pelvis and composed of sheets of eosinophilic polygonal or spindle cell with intracytoplasmic lumen. INI1/SMARCB1 expression was retained. The published cases displayed an *ALK::VCL* fusion if associated with sickle cell disease (49). In our series, the two patients had no history of sickle cell disease, including the case with *ALK::VCL* fusion and the classic pediatric morphology. In the other case with *non-VCL::ALK* gene fusion, the morphology was closer to the case of ALK-rearranged RCC with metanephric adenoma-like morphology described in adults by Kuroda and Hang et al. (49,50). In our cases, *ALK* rearrangement was first confirmed on FISH analysis. The gene fusion transcript was then detected by NGS analysis.

ESCRCCs were first described in 2016 in a cohort of 16 female patients (23). They have also been described in children (24) and have been shown to harbor *TSC1/2* gene mutations in several reports (51,52). Tumors may be multifocal, and only one patient has developed metastasis (24). In our series, one case with a unifocal tumor was suspected. CK20 was negative as in 12% of the Trpkov et al. inaugural cohort tumors (23). Sequencing of *TSC1/2 or MTOR* did not reveal any pathogenic variants. The child was free of disease 111 months after surgery. This unusual case was classified as unclassified RCC.

The other more classic adult tumor types, such as chrRCC, PRCC, CDC, RMC pre-date the 2016 WHO classification and have been previously described in children(4). The diagnosis of PRCC type 2, nomenclature present in the 2016 WHO Classification (4), is more and more controversial with the description of entities such as FH-deficient PRCC and PRCC with reverse polarity. We excluded the diagnosis of FH-deficient PRCC by IHC screening of all cases with papillary morphology and negative *TFE3* FISH and did not observe any morphology evoking PRCC with reverse polarity or other subtypes of RCC with papillary features. Once these two entities are excluded, PRCC type 2 cases include a highly heterogeneous group of tumors sharing papillary architecture and high-grade nuclear features, consistently immunoreactive for AMACR and at least focally for CK7, with retained immunoreactivity for FH and absence of *TFE3* rearrangements (with the bias of the small number of cases undetectable by FISH) ((5,35,36)). They could be better considered as PRCC, NOS, high grade, in keeping with the most recent literature (5). They could represent the papillary counterpart of unclassified RCCs, another group of RCCs for which the application of further molecular studies could be of help in the understanding of their classification, even if in our series the percentage of unclassified RCCs was relatively low due to a thorough immunohistochemical and FISH study coupled with morphology. The application of molecular studies to the group of unclassified RCC and PRCC, NOS, will help improve their classification. Indeed, FISH analyses for *TFE3* rearrangements also fail to detect some less usual translocation partners, like *NONO*, and only the application of techniques like NGS can be practical. Unfortunately, these techniques are costly, time-consuming, and not available in all laboratories for routine purposes.

In this series, multilocular cystic renal neoplasm of low malignant potential, mucinous tubular and spindle cell carcinoma, tubulocystic RCC, or acquired cystic disease associated RCC were not observed.

In our series, radical nephrectomy was performed in 85% of patients, whereas nephron-sparing surgery (NSS) was performed in 15%. In the future, with the development of new surgical techniques, the indication of NSS in pediatric RCC will probably be expanded. In our series, only 53% of the patients had lymph node sampling during surgery. This is in part related to the fact that these tumors affect mainly older children and adolescents who were operated on either by pediatric surgeons following RTSG/SIOP recommendations or adult urologists using different surgical approaches.

At present, no real curative neoadjuvant or adjuvant treatment is available for RCC; the discovery of possible targeted treatments could be improved, taking advance from the reported efficacy of anti-MET tyrosine kinase inhibitors in *MiTF*-TRCC (34). This is also relevant in the management of recurrences, which may occur as late as 20 years after diagnosis.

In this retrospective series, genetic predisposition syndromes were rarely identified and probably underrecognized.

In summary, this study provides new data on RCC subtypes in children and adolescents and underlines not only the central place of the study of *TFE3* and *TFEB* by IHC and FISH analyses for the diagnosis of *MiTF*-RCC but also the crucial importance of an extended immunohistochemical panel for the diagnosis of non-*MITF* translocated RCC, which includes numerous tumoral type with very variable prognosis. We suggest the existence of a ‘pediatric-type TFE3-TRCC’ with a classic morphology. The group of PRCC type 2 could be more appropriately considered as

PRCC, NOS, high grade, deserving further studies for a more accurate classification together with the group of unclassified RCC. An accurate diagnosis is the cornerstone for the most appropriate treatment management in children (given the differential diagnosis of WT in this age group), the patients' inclusion in clinical trials on targeted therapies and preclinical research trials, and genetic counseling of the patients and their families. In our series, many cases of RCCs were not registered in Pediatric Renal Tumor Protocols. Pediatric RCC are currently registered in the SIOP-RTSG UMBRELLA 2016 Study, which will result in more appropriate classification and allow larger studies on the molecular landscape of these tumors (53).

Acknowledgments: We acknowledge the Associazione Bianca Garavaglia for their unstinting support of the Italian studies on pediatric pathology. We also are grateful the Italian Pediatric Renal Tumor Study Group of the GIPOP (Gruppo Italiano di Patologia Oncologica Pediatrica), the AIEOP (Associazione Italiana di Ematologia e Oncologia Pediatrica), Federica Perrone and Elena Tamborini from the Department of Diagnostic Pathology and Laboratory Medicine of the Istituto Nazionale Tumori of Milan, for the NGS analyses, the French Pediatric Renal Tumor Pathology Group, the Société Française du Cancer (SFCE), Julien Masliah from the genetic department of the Institut Curie, and association Enfants et Santé.

Author Contributions: T.D., A.C and P.C. performed study concept and design; A.V, N.R-L., L.M. and A.B. performed molecular and immunohistochemical studies, review and revision of the paper; G.M. and F.S provided clinical information, A.B, S.M., M.B., A.V., J.v.d.B, L.T., M.v.d.H-E. and G.V provided interpretation of data; All authors read and approved the final paper.

References

1. Ahmed HU, Arya M, Levitt G, Duffy PG, Sebire NJ, Mushtaq I. Part II: Treatment of primary malignant non-Wilms' renal tumours in children. Lancet Oncol. 2007;8:842–8.

2. Silberstein J, Grabowski J, Saltzstein SL, Kane CJ. Renal cell carcinoma in the pediatric population: Results from the California cancer registry. Pediatr Blood Cancer. 2009;52:237–41.

3. Sausville JE, Hernandez DJ, Argani P, Gearhart JP. Pediatric renal cell carcinoma. J Pediatr Urol. 2009;5:308–14.

4. Moch H, Cubilla AL, Humphrey PA, Reuter VE, Ulbright TM. The 2016 WHO Classification of Tumours of the Urinary System and Male Genital Organs—Part A: Renal, Penile, and Testicular Tumours. Eur Urol. 2016;70:93–105.

5. Trpkov K, Hes O, Williamson SR, Adeniran AJ, Agaimy A, Alaghehbandan R, et al. New developments in existing WHO entities and evolving molecular concepts: The Genitourinary Pathology Society (GUPS) update on renal neoplasia. Mod Pathol. 2021;34:1392–424.

6. Trpkov K, Williamson SR, Gill AJ, Adeniran AJ, Agaimy A, Alaghehbandan R, et al. Novel, emerging and provisional renal entities: The Genitourinary Pathology Society (GUPS) update on renal neoplasia. Mod Pathol. 2021;34:1167–84.

7. Argani P, Reuter VE, Zhang L, Sung YS, Ning Y, Epstein JI, et al. TFEB-amplified renal cell carcinomas. Am J Surg Pathol. 2016;40:1484–95.

8. Ray S, Jones R, Pritchard-Jones K, Dzhuma K, van den Heuvel-Eibrink M, Tytgat G, et al. Pediatric and young adult renal cell carcinoma. Pediatr Blood

Cancer. 2020;67.

9. Malouf GG, Camparo P, Molini V, Dedet G, Oudard S, Schleiermacher G, et al. Transcription factor E3 and transcription factor EB renal cell carcinomas: Clinical features, biological behavior and prognostic factors. J Urol. 2011;185:24–9.

10. Geller JI, Dome JS. Local lymph node involvement does not predict poor outcome in pediatric renal cell carcinoma. Cancer. 2004;101:1575–83.

11. Geller JI, Argani P, Adeniran A, Hampton E, De Marzo A, Hicks J, et al. Translocation renal cell carcinoma: Lack of negative impact due to lymph node spread. Cancer. 2008;112:1607–16.

12. Rialon KL, Gulack BC, Englum BR, Routh JC, Rice HE. Factors impacting survival in children with renal cell carcinoma. J Pediatr Surg. 2015;50:1014–8.

13. Argani P, Laé M, Ballard ET, Amin M, Manivel C, Hutchinson B, et al. Translocation carcinomas of the kidney after chemotherapy in childhood. J Clin Oncol. 2006;24:1529–34.

14. Schaefer BA, Johnson TS, Hooper DK, Nathan JD, Geller JI. TFE3-positive renal cell carcinoma occurring in three children with dysfunctional kidneys on immunosuppression. Pediatr Transplant. 2017;21:10–3.

15. Bruder E, Passera O, Harms D, Leuschner I, Ladanyi M, Argani P, et al. Morphologic and molecular characterization of renal cell carcinoma in children and young adults. Am J Surg Pathol. 2004;28:1117–32.

16. Selle B, Furtwängler R, Graf N, Kaatsch P, Bruder E, Leuschner I. Population-based study of renal cell carcinoma in children in Germany, 1980-2005: More

frequently localized tumors and underlying disorders compared with adult counterparts. Cancer. 2006;107:2906–14.

17. Rao Q, Chen JY, Wang JD, Ma HH, Zhou HB, Lu ZF, et al. Renal cell carcinoma in children and young adults: Clinicopathological, immunohistochemical, and VHL gene analysis of 46 cases with follow-up. Int J Surg Pathol. 2011;19:170–9.

18. Akhavan A, Richards M, Shnorhavorian M, Goldin A, Gow K, Merguerian PA. Renal cell carcinoma in children, adolescents and young adults: A national cancer database study. J Urol. 2015;193:1336–41.

19. Cajaiba MM, Dyer LM, Geller JI, Jennings LJ, George D, Kirschmann D, et al. The classification of pediatric and young adult renal cell carcinomas registered on the children's oncology group (COG) protocol AREN03B2 after focused genetic testing. Cancer. 2018;124:3381–9.

20. van der Beek JN, Hol JA, Coulomb-l'Hermine A, Graf N, van Tinteren H, Pritchard-Jones K, et al. Characteristics and outcome of pediatric renal cell carcinoma patients registered in the International Society of Pediatric Oncology (SIOP) 93-01, 2001 and UK-IMPORT database: A report of the SIOP-Renal Tumor Study Group. Int J Cancer. 2021;148:2724–35.

21. Abdulfatah E, Kennedy JM, Hafez K, Davenport MS, Xiao H, Weizer AZ, et al. Clinicopathological characterisation of renal cell carcinoma in young adults: a contemporary update and review of literature. Histopathology. 2020;76:875–87.

22. Geller JI, Cost NG, Chi YY, Tornwall B, Cajaiba M, Perlman EJ, et al. A prospective study of pediatric and adolescent renal cell carcinoma: A report

from the Children's Oncology Group AREN0321 study. Cancer. 2020;126:5156–64.

23. Trpkov K, Hes O, Bonert M, Lopez JI, Bonsib SM, Nesi G, et al. Eosinophilic, solid, and cystic renal cell carcinoma. Am J Surg Pathol. 2016;40:60–71.

24. Li Y, Reuter VE, Matoso A, Netto GJ, Epstein JI, Argani P. Re-evaluation of 33 'unclassified' eosinophilic renal cell carcinomas in young patients. Histopathology. 2018;72:588–600.

25. Verkarre V, Morini A, Denize T, Ferlicot S, Richard S. Hereditary kidney cancers: The pathologist's view in 2020. Ann Pathol. 2020;40:148–67.

26. Schmidt LS, Linehan WM. Genetic predisposition to kidney cancer. Semin Oncol. 2016;43:566–74.

27. de la Monneraye Y, Michon J, Pacquement H, Aerts I, Orbach D, Doz F, et al. Indications and results of diagnostic biopsy in pediatric renal tumors: A retrospective analysis of 317 patients with critical review of SIOP guidelines. Pediatr Blood Cancer. 2019;66.

28. Jackson TJ, Williams RD, Brok J, Chowdhury T, Ronghe M, Powis M, et al. The diagnostic accuracy and clinical utility of pediatric renal tumor biopsy: Report of the UK experience in the SIOP UK WT 2001 trial. Pediatr Blood Cancer. 2019;66.

29. Brisse H, de La Monneraye Y, Schleiermacher G. Reply to comment on: The diagnostic accuracy and clinical utility of pediatric renal tumor biopsy: Report of the UK experience in the SIOP UK WT2001 trial [Internet]. Vol. 66, Pediatric Blood and Cancer. John Wiley and Sons Inc.; 2019.

30. Brisse HJ, de la Monneraye Y, Cardoen L, Schleiermacher G. From Wilms to kidney tumors: which ones require a biopsy? [Internet]. Vol. 50, Pediatric Radiology. Springer; 2020. p. 1049–51.

31. Cook A, Lorenzo AJ, Salle JLP, Bakhshi M, Cartwright LM, Bagi D, et al. Pediatric renal cell carcinoma: Single institution 25-year case series and initial experience with partial nephrectomy. J Urol. 2006;175:1456–60.

32. Liu C, Zhang W, Song H. Nephron-sparing surgery in the treatment of pediatric renal cell carcinoma associated with Xp11.2 translocation/TFE3 gene fusions. J Pediatr Surg. 2017;52:1492–5.

33. Malouf GG, Camparo P, Oudard S, Schleiermacher G, Theodore C, Rustine A, et al. Targeted agents in metastatic Xp11 translocation/TFE3 gene fusion renal cell carcinoma (RCC): A report from the Juvenile RCC Network. Ann Oncol. 2010;21:1834–8.

34. Wedekind MF, Ranalli M, Shah N. Clinical efficacy of cabozantinib in two pediatric patients with recurrent renal cell carcinoma. Pediatr Blood Cancer. 2017;64:4–7.

35. Akgul M, Williamson SR, Ertoy Di, Argani P, Gupta S, Caliò A, et al. Diagnostic approach in TFE3-rearranged renal cell carcinoma: A multi-institutional international survey. J Clin Pathol. 2021;74:291–9.

36. Williamson SR, Gill AJ, Argani P, Chen YB, Egevad L, Kristiansen G, et al. Report from the International Society of Urological Pathology (ISUP) Consultation Conference on Molecular Pathology of Urogenital Cancers: III: Molecular Pathology of Kidney Cancer. Am J Surg Pathol. 2020;44:E47–65.

37. Argani P, Zhong M, Reuter VE, Fallon JT, Epstein JI, Netto GJ, et al. TFE3-Fusion Variant Analysis Defines Specific Clinicopathologic Associations Among Xp11 Translocation Cancers. Am J Surg Pathol. 2016;40:723–37.

38. Geller JI, Ehrlich PF, Cost NG, Khanna G, Mullen EA, Gratias EJ, et al. Characterization of adolescent and pediatric renal cell carcinoma: A report from the Children's Oncology Group study AREN03B2. Cancer. 2015;121:2457–64.

39. Argani P. MiT family translocation renal cell carcinoma. Semin Diagn Pathol. 2015;32:103–13.

40. Alrashdi I, Levine S, Paterson J, Saxena R, Patel SR, Depani S, et al. Hereditary leiomyomatosis and renal cell carcinoma: Very early iagnosis of renal cancer in a paediatric patient. Fam Cancer. 2010;9:239–43.

41. Hol JA, Jongmans MCJ, Littooij AS, de Krijger RR, Kuiper RP, van Harssel JJT, et al. Renal cell carcinoma in young FH mutation carriers: case series and review of the literature. Fam Cancer. 2020;19:55–63.

42. Muller M, Ferlicot S, Guillaud-Bataille M, Le Teuff G, Genestie C, Deveaux S, et al. Reassessing the clinical spectrum associated with hereditary leiomyomatosis and renal cell carcinoma syndrome in French FH mutation carriers. Clin Genet. 2017;92:606–15.

43. Toro JR, Nickerson ML, Wei MH, Warren MB, Glenn GM, Turner ML, et al. Mutations in the fumarate hydratase gene cause hereditary leiomyomatosis and renal cell cancer in families in North America. Am J Hum Genet. 2003;73:95–106.

44. Wei MH, Toure O, Glenn GM, Pithukpakorn M, Neckers L, Stolle C, et al. Novel mutations in FH and expansion of the spectrum of phenotypes expressed in families with hereditary leiomyomatosis and renal cell cancer. J Med Genet. 2006;43:18–27.

45. Muller M, Guillaud-Bataille M, Salleron J, Genestie C, Deveaux S, Slama A, et al. Pattern multiplicity and fumarate hydratase (FH)/S-(2-succino)-cysteine (2SC) staining but not eosinophilic nucleoli with perinucleolar halos differentiate hereditary leiomyomatosis and renal cell carcinoma-associated renal cell carcinomas from kidney tum. Mod Pathol. 2018;

46. Ricketts CJ, Shuch B, Vocke CD, Metwalli AR, Bratslavsky G, Middelton L, et al. Succinate dehydrogenase kidney cancer: An aggressive example of the warburg effect in cancer. J Urol. 2012;188:2063–71.

47. Gill AJ. Succinate dehydrogenase (SDH)-deficient neoplasia. Vol. 72, Histopathology. 2018. p. 106–16.

48. Williamson SR, Eble JN, Amin MB, Gupta NS, Smith SC, Sholl LM, et al. Succinate dehydrogenase-deficient renal cell carcinoma: Detailed characterization of 11 tumors defining a unique subtype of renal cell carcinoma. Mod Pathol. 2015;28:80–94.

49. Kuroda N, Trpkov K, Gao Y, Tretiakova M, Liu YJ, Ulamec M, et al. ALK rearranged renal cell carcinoma (ALK-RCC): a multi-institutional study of twelve cases with identi fi cation of novel partner genes. Mod Pathol. 2020;2564–79.

50. Hang JF, Chung HJ, Pan CC. ALK-rearranged renal cell carcinoma with a novel PLEKHA7-ALK translocation and metanephric adenoma-like

morphology. Virchows Arch. 2020;476:921–9.

51. Mehra R, Vats P, Cao X, Su F, Lee ND, Lonigro R, et al. Somatic Bi-allelic Loss of TSC Genes in Eosinophilic Solid and Cystic Renal Cell Carcinoma. Eur Urol. 2018;6–9.

52. Palsgrove DN, Li Y, Pratilas CA, Lin MT, Pallavajjalla A, Gocke C, et al. Eosinophilic solid and cystic (ESC) renal cell carcinomas harbor tsc mutations: Molecular analysis supports an expanding clinicopathologic spectrum. Am J Surg Pathol. 2018;42:1166–81.

53. Van Den Heuvel-Eibrink MM, Hol JA, Pritchard-Jones K, Tinteren H Van, Furtwängler R, Verschuur AC, et al. Position Paper: Rationale for the treatment of Wilms tumour in the UMBRELLA SIOP-RTSG 2016 protocol. Nat Rev Urol. 2017;14:743–52.

Table 1: antibodies/antisera used for immunohistochemistry

ANTIBODIES	CLONE It	CODEX It	SOURCE It	Clone Fr	Codex Fr	Source Fr
TFE3	MRQ-37	354R-16	CELL MARQUE	EPR1159 1	Ab179804	Abcam
Vimentin	V9	M0725	DAKO	V9	M0725	DAKO
Carbonic anhydrase IX	EPR4151	ab108351	Abcam	EPR4151	ab108351	Abcam
AMACR	13H4	M3616	DAKO	EPMU1	AMACR-L-CE	Leica
Keratin 7	OV-TL	M7018	DAKO	OV-TL12/30	NCL-L-CK7-OVTL	Leica
Keratin 19	A53-B/A2	C-6930	SIGMA	A53-B/A2	C-6930	SIGMA
34betaE12 keratin	34BE12	M0630	DAKO	34BE12	M0630	DAKO
CD117	Polyclonal	A4502	DAKO	EP10		Roche
HMB45	HMB45	M0634	DAKO	PA0027	Melanoma-Marker-HMB45	Leica
MelanA	A103	M7196	DAKO	A103	Melan-A	Leica
ALK	5A4	Sc-57024	Santa Cruz Biotechnology	5A4	ALK	Leica
SDHB	Not specified	ab14714	Abcam	21A11AE 7	Ab14714	Abcam
INI1 (BAF47)	25	612111	BD Transduction	25	612111	BD Transduction
FH	J-13	sc-100743	Santa Cruz Biotechnology	J13	sc-100743	Santa Cruz Biotechnology

Legends:

It: Italy; Fr: France; AMACR: alpha-methylacyl-CoA racemase; SDHB: succinate dehydrogenase B; FH: fumarate hydratase

Table 2: Subtypes of 93 pediatric renal cell carcinomas (RCCs) and their frequency

Histotype	Number of cases	% of cases
MiTF-translocation RCC	48	52
Papillary RCC, NOS, high grade	10	11
Papillary RCC, type 1	9	10
Clear Cell RCC	4	4
Chromophobe RCC	3	3
ALK-translocation RCC	2	2
Collecting duct carcinoma	1	1
Renal medullary carcinoma	1	1
SDHB-deficient RCC	1	1
Fumarate Hydratase-deficient RCC	1	1
Unclassified RCC	13	14
Total	93	100

Table 3: Immunohistochemical profiles of 93 pediatric renal cell carcinomas (RCCs)

Tumor type	Number of cases	TFE3	Vimentin	CAIX	CK7	AMACR	CK19	34BE12	HMB45	MelanA	CD117	CD10	FH	SDHB
MiTF-translocated RCC, TFE3 translocated	41	38/38	21/34	16/33	11/37	34/34	11/31	4/31	6/36	2/35	2/34	14/14	16/16	33/33
MiTF-translocated RCC, TFEB translocated	7	2/7	3/5	2/7	1/7	1/7	1/4	1/4	6/7	7/7	2/7	3/4	4/4	6/6
Papillary RCC, NOS, high grade	10	2/10	7/9	3/9	7/10	10/10	6/8	2/8	0/9	0/10	1/9	5/6	10/10	9/9
Papillary RCC, type 1	9	1/8	7/8	1/7	8/8	6/7	3/5	1/5	0/7	0/8	0/9	4/6	6/6	6/6
Clear cell RCC	4	1/2	2/2	3/3	1/3	1/3	1/2	0/2	0/2	0/2	0/2	2/2	1/1	2/2
Chromophobe RCC	3	0/3	0/3	1/2	2/3	0/2	1/1	0/1	0/3	0/3	3/3	0/2	3/3	3/3
ALK-translocated RCC	2	1/2	1/1	0/1	2/2	2/2	1/1	0/1	0/2	0/3	0/1	0/2	NA	2/2
Collecting duct carcinoma	1	1/1	1/1	0/1	1/1	0/1	1/1	1/1	0/1	0/1	0/1	1/1	1/1	1/1
Renal medullary carcinoma	1	0/1	1/1	0/1	1/1	1/1	1/1	1/1	0/1	0/1	1/1	NA	1/1	1/1
SDHB-deficient RCC	1	0/1	1/1	0/1	0/1	1/1	0/1	0/1	0/1	0/1	0/1	1/1	NA	1/1
Fumarate Hydratase-deficient RCC	1	1/1	1/1	0/1	0/1	1/1	0/1	0/1	0/1	0/1	1/1	NA	0/1	1/1
Unclassified RCC	13	6/13	10/13	5/11	3/12	6/12	4/10	3/10	0/12	0/11	0/12	7/8	3/3	10/10

Figure Legends:

Figure 1: TFE3 translocated renal cell carcinoma. Typical short and thick papillae with an admixture of clear and eosinophilic granular cytoplasm and high WHO/ISUP grade as shown on figure 1a and 1b (HES X50 and X100). Psammoma bodies were frequent as shown on figure 1c (HES x100). Some solid areas were also present on figure 1d and 1e (HE x100 an x50). Higher view of large clear and eosinophilic cytoplasm is shown on figure 1f (HE, x200). Keratin 7 was expressed in a third of the cases as shown in figure 1g (HE, X40) with higher view on the top right (HE, X200). AMACR was expressed in all the cases on figure 1h (HE, X 40) with higher view on the top right (HE, X200). CAIX was expressed in about half of the cases and a positive case is shown on figure 1i (HE, X40) with higher view on the top right (HE, X200).

Figure 2: TFEB translocated renal cell carcinoma. Nested, papillary, tubular, and solid architecture are shown on figures 2a, 2b, 2c, 2d (HES, X50). Prominent peripheral lymphoid reaction is shown on figure 2d (HES, X40). A case with prominent large clear cytoplasm is shown on figures 2e, 2f (HES, X100). Tumoral cells focally expressed CD10 as shown on figure 2g (CD10, X40) with higher view on the top right (HE, X200). HMB45 on figure 2h (HMB45, X40) with higher view on the top right (HE, X200). Melan-A on figure 2i (Melan A, X40) with higher view on the top right (HE, X200).

Figure 3: Oncocytic PRCC round nuclei with a prominent nucleolus is shown on figure 3a (HES, X40). Typical chromophobe renal cell carcinoma composed of nests or trabeculae of eosinophilic cells with granular cytoplasm and well-demarcated cell membranes is shown on figure 3b (HES, X200). Adult type CCRCC with a nested architecture of clear cells is shown in figure 3c (HES, X40). CCRCC with morphology suspect of Clear Cell PRCC composed of clear cylindrical cells organized in tubules and papillae is shown on figures 3d and 3e (HES, X40 and X100). CAIX strong and diffuse expression on figure 3f (CAIX, X40 and X100). ALK-translocated RCCs with metanephric adenoma-like morphology and with sheets and cords of eosinophilic/oncocytic syncytial cells with moderate nuclear polymorphism and mild

atypia are shown on figures 3g, 3g (HE, X100). ALK cytoplasmic with membranous reinforcement expression is shown on figure 3i (ALK, X200).

Figure 4: SDHB-deficient RCC with an acinar architecture, a mucinous stroma and eosinophilic cells with low-grade nuclei is shown on figures 4a and 4b (HE, X100 and 200). SDHB expression was lost as shown on figure 4c (SDHB, X200). FH-deficient RCC with a tubular-papillary, microcystic and acinar architecture is shown on figure 4d (HES, X100). Tumoral cells were lightly eosinophilic with nuclei containing a cherry red nucleolus with a perinucleolar clarification as shown on figure 4e (HES, X400). FH expression was lost by tumor cells whereas it was retained by vascular cells within the tumor on figure 4f (FH, X100). Unclassified RCC with characteristic suggestive of Eosinophilic solid and cystic carcinoma (ESCRCC) with solid, tubular and acinar architecture made of eosinophilic granular cells with multinucleated tumoral cells is shown on 4g (HES, X100). AMACR was diffusely expressed as shown on figure 4h (AMACR, X100) and CD10 showed a typical apical expression pattern on figure 4i (CD10, X200).

Supplementary figure 1: PRCC type 1 with typical morphology characterized by thin papillae lined by small clear to eosinophilic cells as shown on supplementary figure 1a (HES, X40). PRCC, NOS, high grade with papillary architecture with eosinophilic cytoplasm is shown on supplementary figure 1b (HES, X200). Oncocytic PRCC with tubulo-papillary architecture with large oncocytic tumoral cells is shown on supplementary figure 1c (HES, X40). Collecting duct carcinoma with large eosinophilic and atypical cells organized in tubules, isolated cells, or small sheets in a stroma reaction is shown on supplementary figure 1d (HE, X100). Medullary carcinoma with trabecular or small sheets of atypical cells with rhabdoid features in a fibrous stroma infiltrated by a polymorphous inflammatory and high mitotic activity and numerous apoptosis is shown on supplementary figure 1e (HES, X100). INI1/SMARCB1 loss of expression is shown on supplementary figure 1f (INI1/SMARCB1, X 100). Unclassified RCC with various papillary architectural patterns and various cell morphology are shown on supplementary figure 1g, 1h, 1i (HES, X40, X100 and X200).

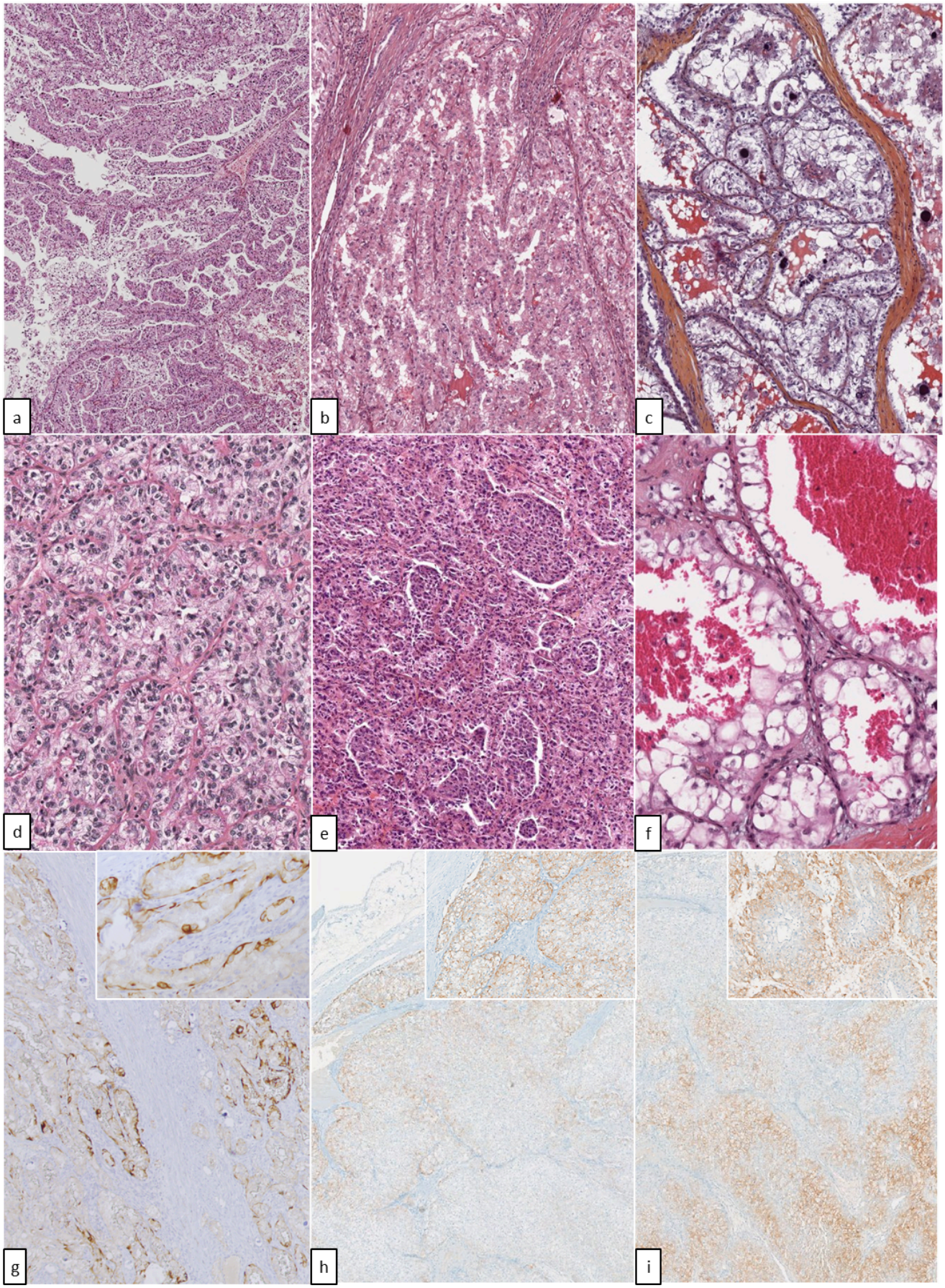

HIS_14634_fig1.png

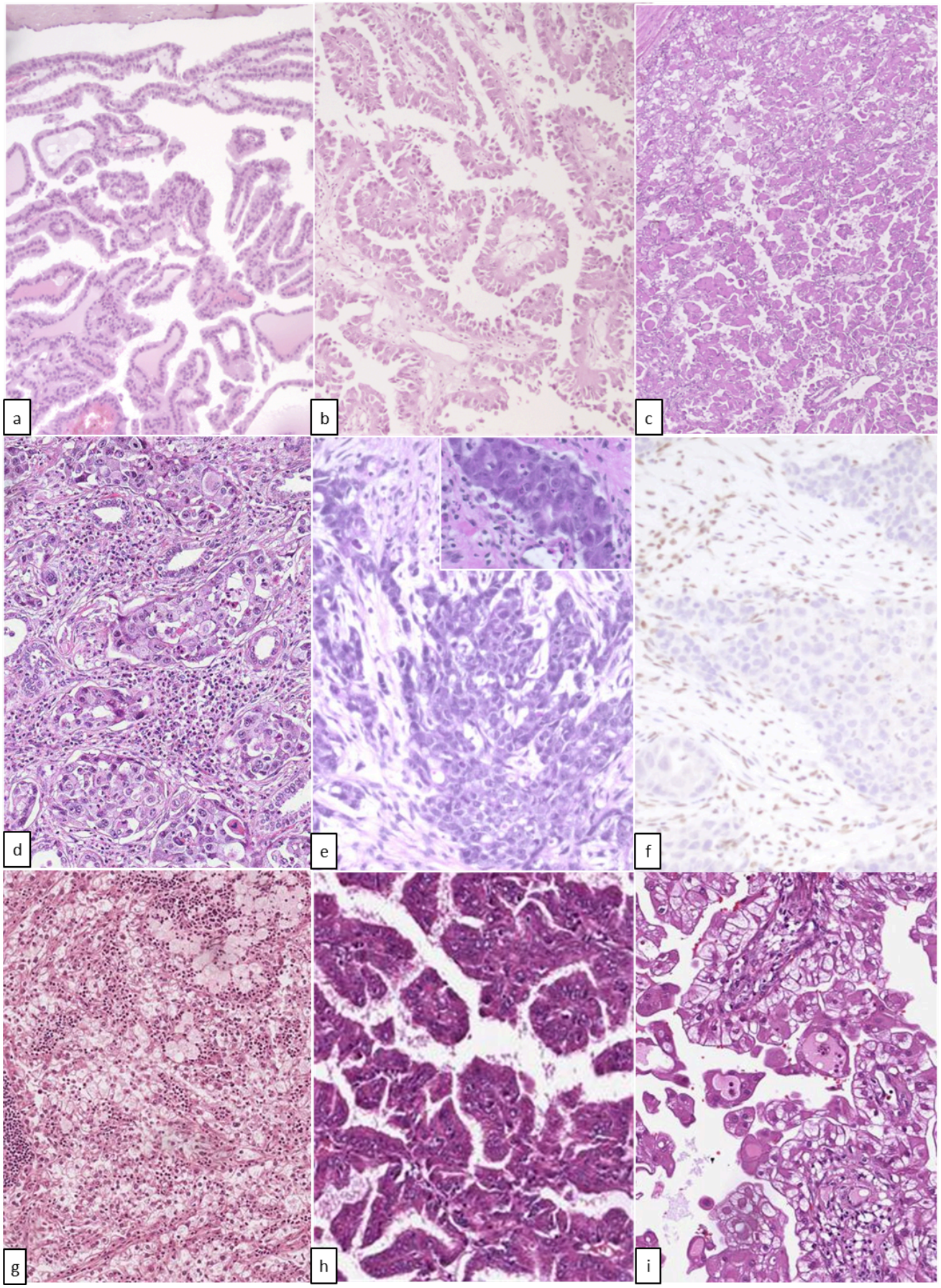

HIS_14634_fig1s.png

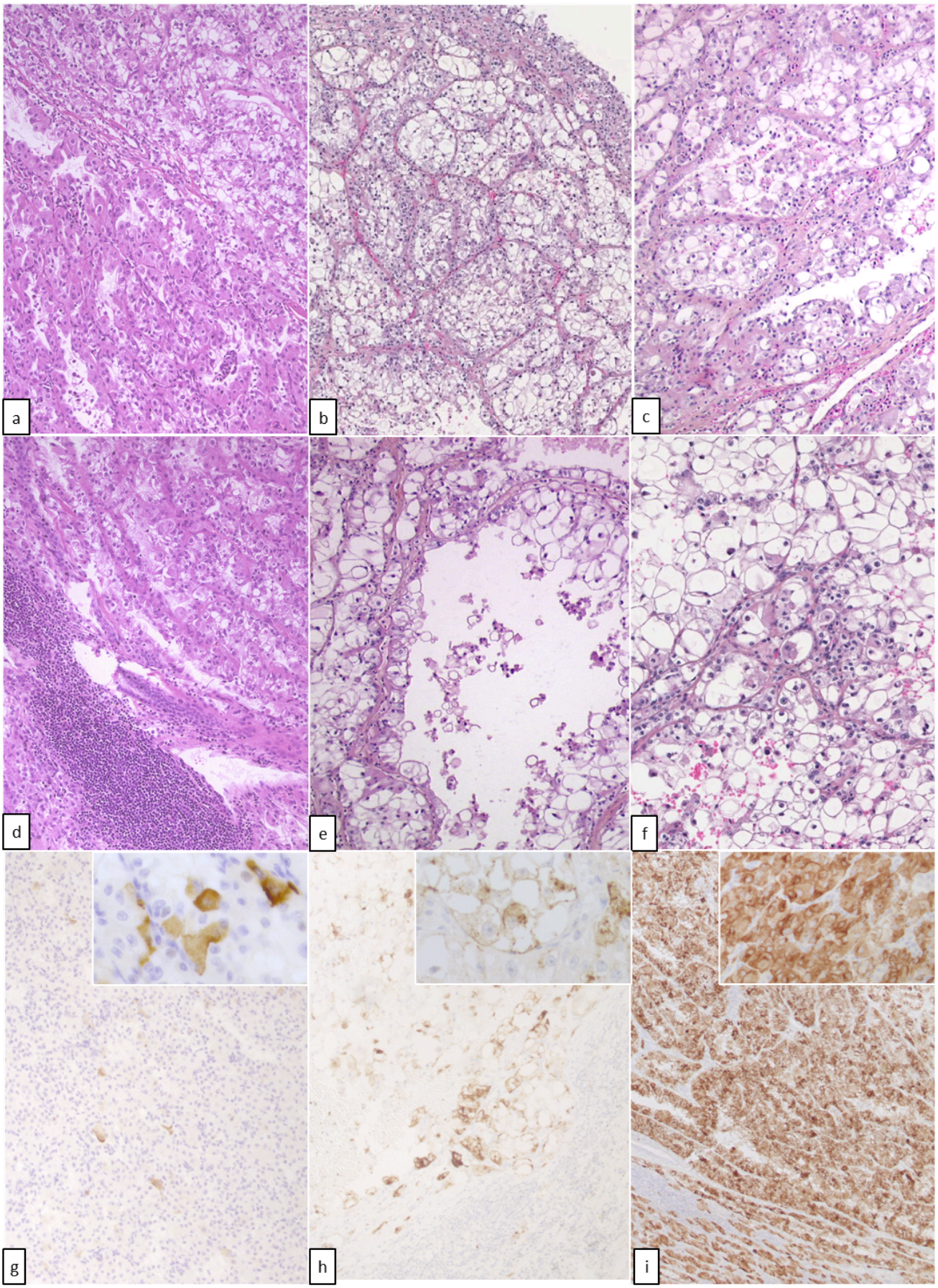

HIS_14634_fig2.png

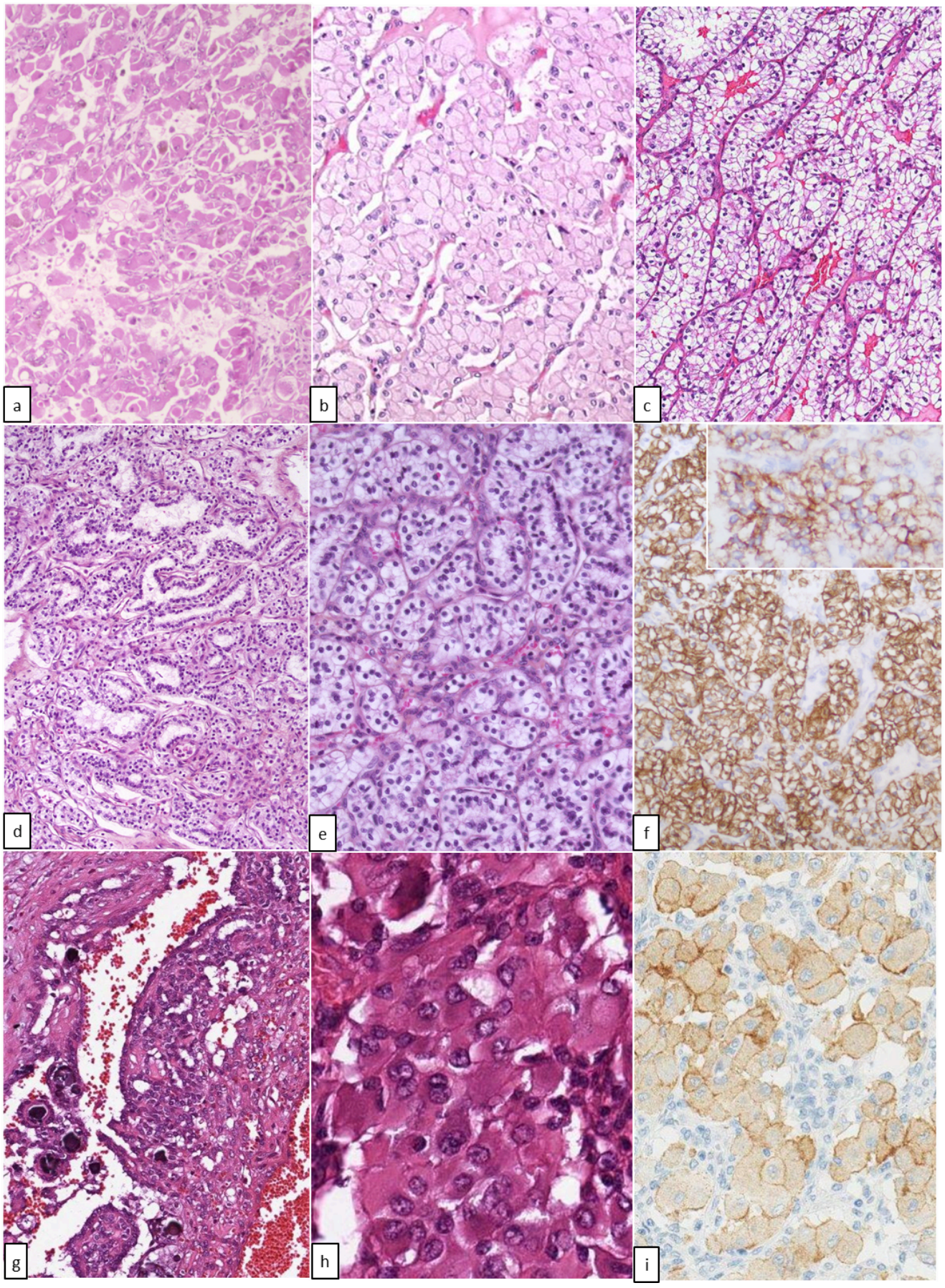

HIS_14634_fig3.png

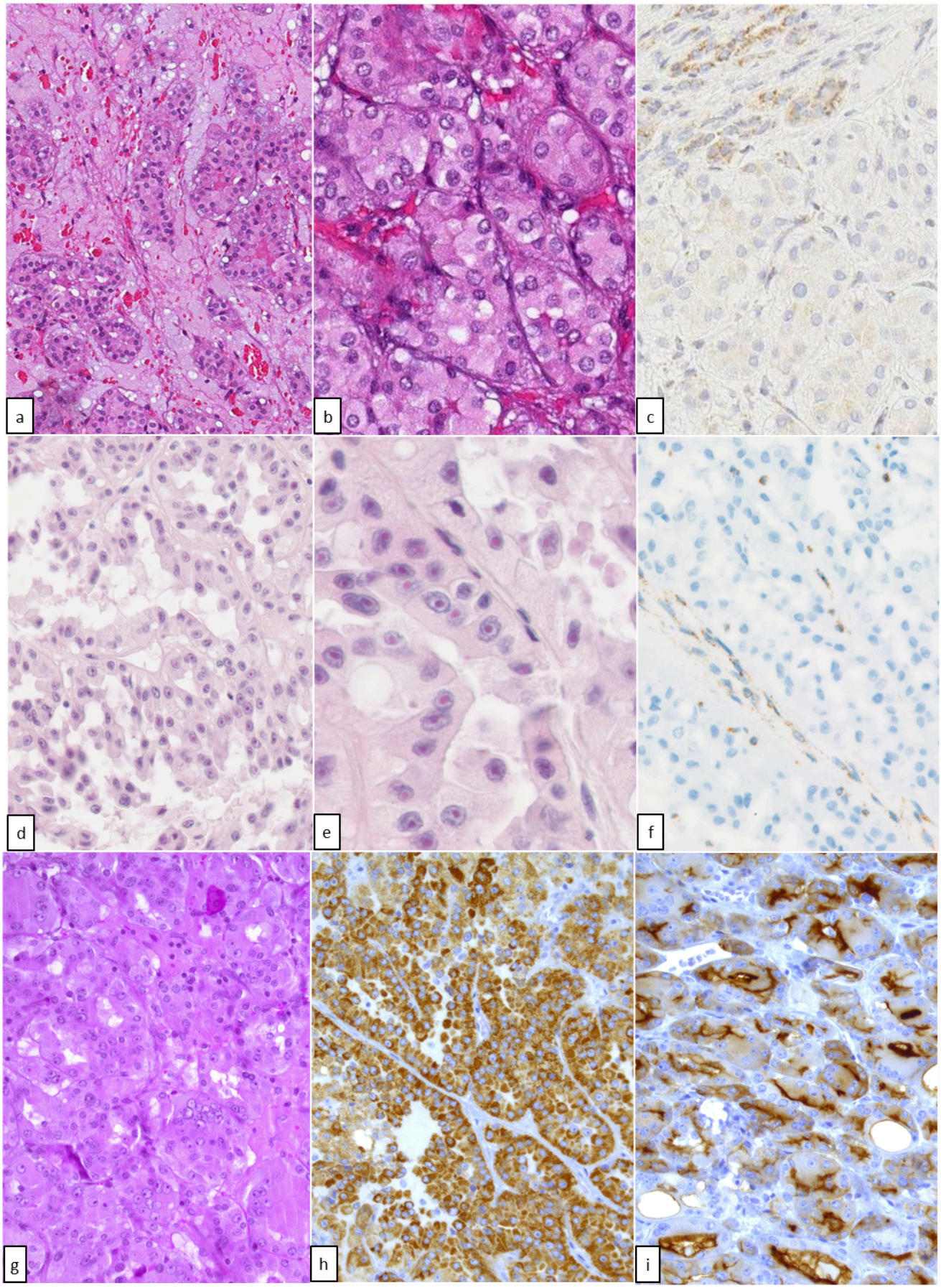

HIS_14634_fig4.png